

# Competition between $X\cdots H\cdots Y$ Intramolecular Hydrogen Bonds and $X\cdots Y$ ( $X = O, S,$ and $Y = Se, Te$ ) Chalcogen–Chalcogen Interactions

Pablo Sanz, Manuel Yáñez, and Otilia Mó\*

Departamento de Química, C-9, Universidad Autónoma de Madrid, Cantoblanco, 28049-Madrid, Spain

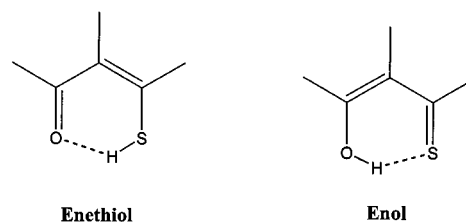
Received: November 29, 2001; In Final Form: February 28, 2002

High-level G2(MP2) ab initio and B3LYP/6-311+G(3df,2p) density functional calculations have been carried out for a series of  $\beta$ -chalcogenovinylaldehydes,  $HC(=X)-CH=CH-CYH$  ( $X = O, S; Y = Se, Te$ ). Our results indicate that for  $X = O, S$  and  $Y = Se, Te$ , the  $O-H\cdots Se$  and the  $S-H\cdots Se$  intramolecular hydrogen bonds compete in strength with the  $O\cdots Se$  and the  $S\cdots Se$  interaction, while the opposite is found for the corresponding tellurium-containing analogues. The different strength of  $O-H\cdots Se$  and  $O\cdots H-Se$  intramolecular hydrogen bonds explains why the chelated *enolic* and *keto* forms of selenovinylaldehyde are very close in energy, although *enol*-tautomers are estimated to be about 10 kcal mol<sup>-1</sup> more stable than *keto*-tautomers. The situation is qualitatively similar for selenothiovinylaldehyde, although the  $S-H\cdots Se$  and  $S\cdots H-Se$  intramolecular hydrogen bonds (IHBs) are weaker and much closer in strength, and the energy gap between *enethiol*- and *thione*-tautomers also smaller. The relative strengths of the  $X-H\cdots Te$  and  $X\cdots H-Te$  ( $X = O, S$ ) IHBs, are very similar to those of the corresponding selenium analogues. However, there are dramatic differences as far as the  $X\cdots Y$  ( $X = O, S; Y = Se, Te$ ) interactions are concerned, which for Se-derivatives are rather small, while for Te-compounds are very strong. An analysis of these chalcogen-chalcogen interactions indicates that both, the electrostatic and the dative contributions are smaller for Se- than for Te-derivatives. In the latter, the electrostatic component clearly dominates when  $X = O$ , while the opposite is found for sulfur-containing derivatives. We have also shown that these two components are entangled in some manner, in the sense that strong electrostatic interactions favor the  $n_O-\sigma^*_{YH}$  (or  $n_S-\sigma^*_{YH}$ ) dative interaction. The proton-transfer processes in species with IHBs were also investigated.

## Introduction

Intramolecular hydrogen bonds (IHBs) play an important role in chemistry, mainly in processes which take place in the gas phase.<sup>1–3</sup> These weak bonds are responsible for the enhanced stability of chelated structures with respect to open ones, as it is the case for instance in malonaldehyde.<sup>4–8</sup> On the other hand, the formation of these chelated forms has a nonnegligible effect on the intrinsic reactivity of the system, as it has been shown, for instance, concerning the intrinsic basicity and acidity of tropolone<sup>9</sup> or the intrinsic basicity of resorcinol.<sup>10</sup> In other cases, the formation of an intramolecular hydrogen bond in the protonated species is responsible for a significant enhancement of the intrinsic basicity of the system.<sup>11</sup> As a consequence, these bonds have received a great deal of attention, both from the experimental and the theoretical points of view. However, most of these efforts concentrate on the study of systems, such as malonaldehyde or tropolone,<sup>12–16</sup> where both the hydrogen bond donor and the hydrogen bond acceptor are oxygen atoms. In our group we have been interested in the study of systems, such as thiomalonaldehyde (TMA)<sup>17,18</sup> where an asymmetric prototropic tautomerism can be observed. The fact that the hydrogen bond donor is different from the hydrogen bond acceptor opens the possibility of having a mixture of rapidly interconverting *enol*- and *enethiol*-tautomeric forms. As a matter of fact, the existence of both tautomers has been well-established by means of UV,<sup>19</sup> UV photoelectron,<sup>20</sup> IR,<sup>19</sup> and <sup>1</sup>H NMR spectroscopies.<sup>21,22</sup> Consistently, high-level ab initio calculations predict both tautomers to be nearly degenerate.<sup>17</sup> This result should be unexpected in the absence of the  $S\cdots H\cdots O$  IHB. In

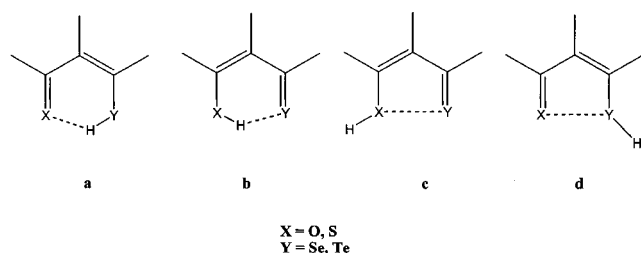
## SCHEME 1



fact, TMA-tautomers containing  $S-H$  and  $C=O$  bonds are systematically 5–10 kcal mol<sup>-1</sup> more stable than those with  $O-H$  and  $C=S$  bonds.<sup>17</sup> However, despite this, the chelated *enol* (see Scheme 1) is only 0.2 kcal mol<sup>-1</sup> less stable than the chelated *enethiol*, due to the presence of a quite strong  $O-H\cdots S$  intramolecular hydrogen bond. Also importantly, this compound and its derivatives have been successfully used as model systems to investigate ultrafast hydrogen transfer through pulsed lasers.<sup>23–25</sup>

To the best of our knowledge there is, however, a complete lack of information regarding intramolecular hydrogen bonds in which the hydrogen bond acceptor is Se or Te, or where the hydrogen bond donor is a  $Se-H$  or a  $Te-H$  group, and only very recently, a theoretical study on intermolecular hydrogen bonds involving  $H_2CSe$  has been published.<sup>26</sup> Therefore the aim of this paper is the characterization of the IHB in the series of compounds depicted in Scheme 2. These systems present an added interest since, as it has been shown many years ago<sup>27–29</sup> and more recently by Minyaev and Minkin<sup>30,31</sup> they exhibit specific attractive forces between the two chalcogen atoms involved. Also recently, Komatsu et al.<sup>32</sup> showed that <sup>17</sup>O and

## SCHEME 2



$^{77}\text{Se}$  NMR spectroscopic data provide strong evidence for intramolecular nonbonded interaction between Se and O in hydroxy-selenenyl compounds. These interactions seem to play also an important role in some reaction mechanisms.<sup>33</sup> Hence, one of the aims of this paper is to investigate the competition between  $X\text{-H}\cdots\text{Y}$  (or  $X\cdots\text{H}-\text{Y}$ ) IHBs (structures **a** and **b** in Scheme 2) and  $\text{Y} \rightarrow \text{X}$  (or  $\text{X} \rightarrow \text{Y}$ ) chalcogen-chalcogen-nonbonded interactions (structures **c** and **d** in Scheme 2), which, to the best of our knowledge, has not been analyzed before. In addition to the structures included in Scheme 2 we shall consider in our analysis the possible open forms in which none of the two aforementioned interactions are possible.

## Computational Details

The relative stability of the different tautomers of the compounds under investigation was evaluated by using the G2(MP2) theory.<sup>34</sup> This theory provides total energies of an effective QCISD(T)/6-311+G(3df,2p) quality, and it has been found to be quite reliable in the study of similar systems having intramolecular hydrogen bonds.<sup>17,18</sup>

To apply this theoretical scheme to Se-containing compounds the 6-31G(d) and the 6-311+G(3df,2p) basis set expansions developed by Curtiss et al.<sup>35</sup> have been used. No G2-type extended basis sets have been reported for Te so far. Therefore, to treat Te- and Se-containing compounds on equal footing we have optimized the G2-type basis for Te following an analogous procedure to that reported in the literature to obtain similar basis sets for I,<sup>36</sup> Sb,<sup>37</sup> or Sn.<sup>38</sup>

Among the different effective core potentials which have been proposed in the literature for Te we have chosen the SKBJ relativistic potential of Stevens et al.,<sup>39</sup> because it was found to perform very well for other forth row elements.<sup>37,38</sup> This ECP approach accounts for the most important relativistic effects. In this procedure the valence electrons of third and fourth-row atoms are described by using a (5s,5p)/[2s,2p] basis set which implies a [4,1] contraction scheme, and adopts a typical shell-structure ( $\alpha_s = \alpha_p$ ).

Taking into account that in the standard G2 formalism,<sup>40</sup> the geometry optimizations are performed using a 6-31G(d) basis set, the polarization d function to be included in geometry optimizations was optimized through calculations at the MP2 level for  $\text{TeH}_2$ , on its experimental geometry,<sup>41</sup> using a 31G basis for the hydrogen atoms and the aforementioned [4,1] contraction for Te. Hereafter, for the sake of simplicity this [4,1] + d basis for Te, to be used in conjunction with a 6-31G-(d) basis set for first and second row atoms, will be named for extension 6-31G(d).

To obtain for Te the supplementary diffuse s, p components and the d, f polarization functions required in G2 calculations, we have completely uncontracted the original scheme. Using this (5s,5p)[11111/11111]-uncontracted basis for Te and a 311G(p) basis set for hydrogen and the  $\text{TeH}_2$  molecule as a model system, the exponent of the d polarization function for

**TABLE 1: Variationally Optimized Exponents of the d and f Polarization Functions and the s,p Diffuse Functions for the Augmentation of the Valence Basis Set in ECP Calculations of Te-Containing Compounds**

ECP	d <sup>a</sup>	d <sup>b</sup>	f	sp
SKBJ	0.2248	0.21653	0.30727	0.02542

<sup>a</sup> Values to be used with the [4,1] contraction valence basis sets in geometry optimizations. <sup>b</sup> Values to be used with the uncontracted [11111,11111] valence basis sets in single-point high-level calculations.

Te was optimized through QCISD(T) calculations. To create multiple sets of d functions from a single optimized function we have adopted the usual procedure, in which the new exponents are obtained as multiples,  $n\alpha_d$ , or fractions,  $\alpha_d/n$ , of the single optimized exponent  $\alpha_d$ . We have explored several factors and, although the differences are very small when the value of  $n$  is changed, the best results are obtained for  $n = 1.5$  for the (2d) splitting and  $n = 2$  for the (3d) splitting, which coincide with the values normally used for fourth-row elements. This (5s,5p,1d) basis for Te, to be used in conjunction with 6-311G(d,p) basis sets for first- and second-row atoms, will be designated hereafter as 6-311G(d,p) for the sake of consistency.

With the 6-311G(d,p) basis so defined and using the 6-31G(d)-optimized geometry of  $\text{TeH}^-$  as model system, the set of diffuse s, p functions for Te (with the constraint  $\alpha_s = \alpha_p$ ), were optimized at the QCISD(T) level of theory. The set of f polarization functions was optimized using  $\text{TeH}_2$  at the QCISD(T)/6-311G(2df,p) level. The values of the different exponents obtained are given in Table 1. Hence, hereafter a 6-311+G(3df,2p) basis set for Te, will designate the use of the SKBJ ECP together with a (6s,6p,3d,1f) basis set.

Although in the standard G2(MP2) procedure the geometries are optimized at the MP2(full)/6-31G\* level, in our case we have used a 6-31+G(d,p) basis set because diffuse functions are needed to appropriately describe hydrogen bonds. Taking into account that for large systems the G2(MP2) procedure can become prohibitively expensive we have considered it of interest to assess the reliability of the B3LYP density functional theory approach<sup>42</sup> which can be easily extended to the treatment of much larger systems. For this purpose we have compared the results obtained at the G2(MP2) level of theory with those obtained when the B3LYP method is used. The B3LYP method combines Becke's three-parameter nonlocal hybrid exchange potential<sup>43,44</sup> with the nonlocal correlation functional of Lee, Yang, and Parr.<sup>45</sup> In these DFT calculations, the geometries and harmonic vibrational frequencies were obtained at the B3LYP/6-31+G(d,p) level, while the final energies were evaluated by means of single-point B3LYP/6-311+G(3df,2p) calculations.

The bonding characteristics of the different tautomers were analyzed by using two alternative procedures, namely the atoms in molecules (AIM) theory of Bader<sup>46</sup> and the natural bond order (NBO) analysis of Weinhhold et al.<sup>47</sup> The first method is based on a topological analysis of the electron charge density and its Laplacian. Within this approach we have located the different bond critical points whose charge density is a good indication of the strength of the linkage. Besides, we have also evaluated the contour maps of the energy density  $H(\mathbf{r})$ , which would help to characterize the nature of the different linkages. It has been established<sup>48</sup> that, in general, the internuclear regions characterized by negative values of  $H(\mathbf{r})$  correspond to covalent interactions, while positive values are typical of interactions between closed-shell systems as in ionic bonds or hydrogen bonds.

The NBO analysis will allow us to obtain reliable charge distributions, as well as to evaluate quantitatively the intramolecular attractive orbital interactions which would be responsible

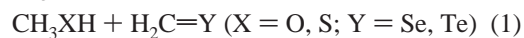
for the stability of *c*- and *d*-type structures (See Scheme 2). These analyses will be complemented with those carried out in terms of the lengthening or shortening of the bond lengths and in terms of the shifting of the corresponding stretching frequencies.

## Results and Discussion

The optimized geometries of the different conformers of the compounds under investigation have been schematized in Figure 1, which shows also their relative stabilities. To make our discussion more systematic, the following nomenclature will be adopted hereafter. The different compounds will be identified by naming the two chalcogen atoms YX involved followed by *a* if the hydrogen atom is attached to the lighter chalcogen atom and by *b* if the hydrogen atom is attached to the heavier one. For instance, in the case of oxygen-containing compounds structures *a* would correspond systematically to the *enol*-tautomers and structures *b* to the *keto* ones. The different tautomers of each type will be identified by adding a number which will follow the stability order. Hence, for instance, **SeOa1** designates the most stable *enol* form of the  $\beta$ -selenovinylaldehyde, while **SeOb1** would name the most stable *keto* (*selenol*) conformer. In addition to the chelated structures which present either an IHB or a chalcogen-chalcogen interaction, there are many noncyclic conformers. Although many of these open conformers have been investigated, in what follows, and for the sake of conciseness, we will constrain our discussion to the most stable of each type (*a* or *b*).

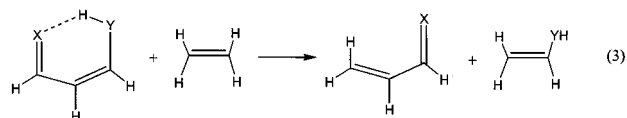
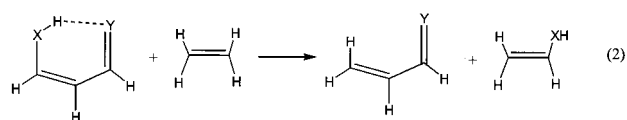
The values reported in Figure 1 indicate that the B3LYP/6-311+G(3df,2p) approach yields systematically the same stability order as the G2(MP2) method. The calculated relative stabilities are also very similar, the differences being typically smaller than 1 kcal mol<sup>-1</sup>. Hence, the more expensive G2(MP2) calculations have been restricted to a limited set of test cases which permitted us to assess the reliability of the B3LYP approach.

**Relative Stabilities. Selenium Compounds with X = O.** Even though the structures containing Se–H and C=O bonds (*b*-type tautomers) should be more stable than those containing O–H and C=Se bonds (*a*-type tautomers), the most stable conformer of the selenovinylaldehyde, **SeOa1**, corresponds to an *enol* structure which presents a O–H $\cdots$ Se intramolecular hydrogen bond. Very close in energy lies the corresponding *keto* form **SeOb3**, which presents a O $\cdots$ HSe IHB. It is worth noting that according to these results selenovinylaldehyde resembles closely the sulfur analogue thiomalonaldehyde. Indeed, for TMA, the chelated *enol*-tautomer, stabilized by O–H $\cdots$ S IHB, and the chelated *enethiol*-tautomer, stabilized by an O $\cdots$ H–S IHB, were found to be practically degenerate<sup>17</sup> even though the *enols* should be much less stable than the corresponding *enethiols*. This seems to indicate, on one hand, that the selenocarbonyl group is as good a hydrogen bond acceptor as the thiocarbonyl group, in line with the fact that selenocarbonyl compounds were predicted to have an intrinsic basicity rather similar to that of the corresponding thiocarbonyl analogues.<sup>49</sup> On the other hand, also similarly to what was found for TMA,<sup>17</sup> the OH $\cdots$ Se IHB in **SeOa1** species should be much stronger than the O $\cdots$ HSe one in **SeOb3**, to counterbalance the enhanced intrinsic stability of the *selenol*-tautomer. This can be analyzed on more quantitative grounds. The enhanced stability of the *b*-type *selenol* structures with respect to the *a*-type *enolic* forms can be estimated by comparing the atomization energies of H<sub>2</sub>C=O + CH<sub>3</sub>SeH with those of CH<sub>3</sub>OH + H<sub>2</sub>C=Se, i.e., by estimating the energy associated with the isodesmic reaction:



At the G2(MP2) level reaction 1 for X = O and Y = Se, is predicted to be endothermic by 13.6 kcal mol<sup>-1</sup>, (See Table 2), ratifying the enhanced stability of the *b*-type forms. This result is also corroborated by the fact that the *b*-type open structures (which present neither IHBs nor chalcogen-chalcogen interactions) are systematically 5–10 kcal mol<sup>-1</sup> more stable than the corresponding *a*-type tautomers (See Figure 1).

The energy associated with an intermolecular hydrogen bond can be easily estimated taken as a reference the energy of the isolated interacting units. However, this is not the case when dealing with intramolecular hydrogen bonds because it is not possible to define an appropriate reference. In our case, it would be enough, however, to estimate the relative strength of the OH $\cdots$ Se IHB with respect to the O $\cdots$ HSe IHB, and this can be reasonably achieved by using the following isodesmic reactions:



The G2(MP2) calculated energies are summarized in Table 3. It can be observed that for X = O and Y = Se, both reactions are endothermic, reflecting the stabilizing effect of both IHBs. However, in agreement with our previous assumption, the O–H $\cdots$ Se IHB is estimated to be more than 9 kcal mol<sup>-1</sup> more stable than the O $\cdots$ H–Se one. This difference practically counterbalances the energy gap between *b*-type and *a*-type forms mentioned above, and as a consequence, the **SeOa1** and the **SeOb3** conformers are found to be very close in energy.

Another important finding is that the second local minimum of the potential energy surface is the **SeOb1** structure characterized by a O $\cdots$ Se stabilizing intramolecular interaction already described by Minyaev and Minkin.<sup>30,31</sup> Nevertheless, the energy difference between this chelated structure and the most stable open form, **SeOb2**, is rather small indicating that this stabilization energy is not very large, being of the same order as the energy of the O $\cdots$ H–Se IHB.

Hence, the important conclusion is that in SeO-derivatives, the O–H $\cdots$ Se IHB is strong enough to counterbalance not only the intrinsic enhanced stability of the *b*-type forms, but also the stabilizing O $\cdots$ Se interaction present in form **SeOb1** or the O $\cdots$ H–Se IHB in structure **SeOb3**. It is also worth noting that the chalcogen-chalcogen (O $\cdots$ Se) interaction for *a*-type compounds is repulsive rather than attractive as in *b*-forms, as reflected by the low stability of the **SeOa3**-tautomer with respect to the most stable open analogue, **SeOa2**.

The OH lengthening in **SeOa1** with respect to the open structure (**SeOa2**) is much greater (0.043 Å) than the one undergone by the Se–H bond (0.004 Å) in **SeOb3** with respect to the corresponding open structure **SeOb2**. This clearly indicates that the O–H $\cdots$ Se IHB in the global minimum is much stronger than the O $\cdots$ H–Se IHB in **SeOb3**. Concomitantly, the OH stretching frequency in the global minimum appears red shifted by 894 cm<sup>-1</sup> with respect to **SeOa2**, while the red shifting of the Se–H stretching frequency in **SeOb3** with respect

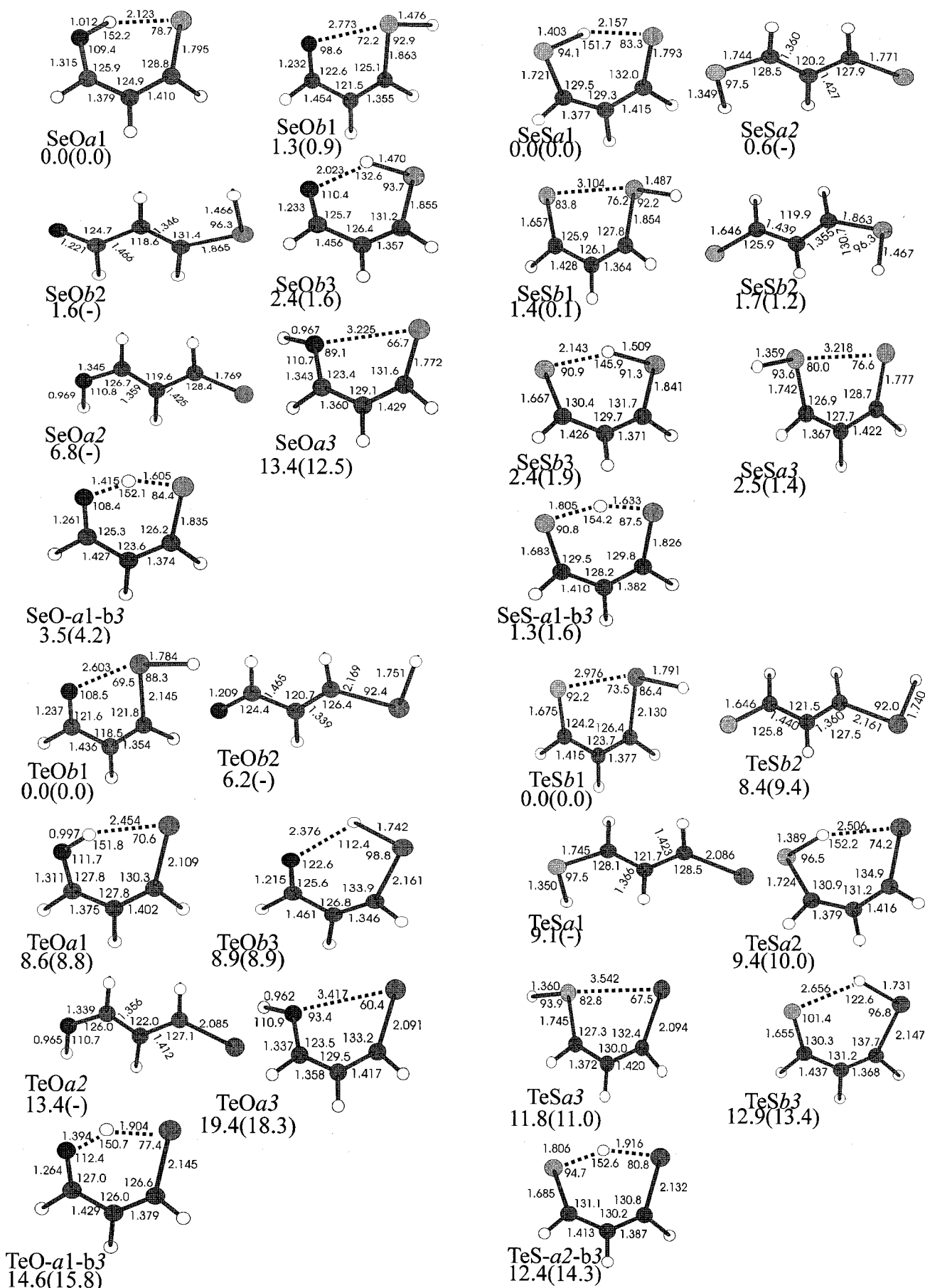


**Figure 1.** B3LYP/6-311G(d,p)-optimized geometries of the different systems under investigation. Bond lengths in Å and bond angles in degrees. Relative energies (kcal mol<sup>-1</sup>) have been evaluated at the B3LYP/6-311\*G(3df,2p) and G2(MP2) levels of theory. The latter ones correspond to the values within parentheses.

**TABLE 2: Energies of the Isodesmic Reaction  $\text{H}_2\text{CX} + \text{CH}_3\text{YH} \rightarrow \text{CH}_3\text{XH} + \text{H}_2\text{CY}$  (X = O, S; Y = Se, Te) Evaluated at the G2(MP2) Level of Theory<sup>a</sup>**

Y = Se		Y = Te	
X = O	X = S	X = O	X = S
13.6	1.9	13.5	1.8

<sup>a</sup> Values in kcal mol<sup>-1</sup>.

to **SeOb2** is only 44 cm<sup>-1</sup> (See Table 4). It is also worth noting, by comparing the structures of **SeOa1**- and **SeOa2**-tautomers, that the formation of the OH $\cdots$ Se IHB leads to a shortening of the C–O bond and to a lengthening of the C=Se linkage. Consistently, on going from **SeOa2** to **SeOa1**, the C–O stretching frequency appears blue shifted by 26 cm<sup>-1</sup>, while the C=Se stretching frequency shifts 178 cm<sup>-1</sup> to the red. Similar changes, although smaller are observed when an O $\cdots$ H–Se IHB is formed, i.e., on going from **SeOb2** to **SeOb3**. Hence, in general the C–XH bond of the hydrogen bond donor group becomes reinforced when the IHB is formed, while the C=Y bond of the hydrogen bond acceptor group becomes weakened. These geometrical distortions can be easily explained taking into account that in the limit, i.e., when the proton has been completely transferred, the C–XH bond will change into a C=X linkage, while the C=Y bond will become a C–YH linkage.

*Selenium Compounds with X = S.* The same stability order discussed above for the chelated structures is observed when oxygen is substituted by sulfur. For the selenothiovinylaldehyde, again the most stable conformer, **SeSa1**, is the one exhibiting a S–H $\cdots$ Se IHB, while the second one in stability, **SeSb1**, presents a S $\cdots$ Se interaction. Also in this case the energy gap between the *enethiol*-tautomer **SeSa1** (with a S–H $\cdots$ Se IHB) and the *selenol*-tautomer **SeSb3** (with a S $\cdots$ H–Se IHB) is quite small. Despite these analogies there are significant quantitative differences between oxygen and sulfur-derivatives. As shown in Table 2 for sulfur-containing systems the enhanced stability of the *b*-type (*enethiol*) tautomers with respect to the *a*-type (*selenol*), as measured by the endothermicity of reaction 1 reduces to only 1.9 kcal mol<sup>-1</sup>. At the same time, as shown in Table 3, the S–H $\cdots$ Se IHBs is not only much more weaker than the O–H $\cdots$ Se IHB but only slightly stronger (about 1.6 kcal mol<sup>-1</sup>) than the S $\cdots$ H–Se one. So at the end, as it was found for oxygen-containing compounds, these effects, although significantly smaller, almost cancel each other, and thus, species **SeSa1** and **SeSb3** are very close in energy. The rather small difference between the **SeSb1** and **SeSb2** forms indicates that also in selenothiovinylaldehydes the chalcogen–chalcogen interaction is weak. Also, as a consequence of the weakness of the S $\cdots$ H–Se IHB, the open form **SeSa2** is predicted to be slightly more stable than the **SeSb1** chelated structure.

The fact that in this case the S–H $\cdots$ Se and the S $\cdots$ H–Se IHBs are close in strength is also mirrored in the charge density at the corresponding bond critical point (see Table 5), which is only slightly higher for the former. Consistently the lengthening of the S–H and the Se–H bonds upon formation of the IHB (0.054 Å and 0.042 Å, respectively) is not very different. Coherently, on going from **SeSa2** to **SeSa1** the S–H stretching frequency appears red shifted by 681 cm<sup>-1</sup>, while on going from **SeSb2** to **SeSb3** the Se–H stretching shifts 464 cm<sup>-1</sup> to the red. Changes in the bond lengths and stretching frequencies of the C–XH and the C=Y bond upon formation of the IHB are also similar to those discussed above for the oxygen-derivatives (See Figure 1 and Table 4).

*Tellurium Compounds.* The situation changes completely when dealing with tellurium-containing compounds. In this case

the most stable conformer corresponds always to a *b*-type form, namely **TeOb1** and **TeSb1**, stabilized by a X $\cdots$ Y chalcogen–chalcogen interaction. Nevertheless, as it was the case for selenium-derivatives, for X = O the most stable *a*-type structure, **TeOa1**, is stabilized by an O–H $\cdots$ Te IHB. For X = S, however, and due to the weakness of the S–H $\cdots$ Te IHB (See Table 3), the **TeSa1** open form is predicted to be slightly (0.3 kcal mol<sup>-1</sup>) more stable than the chelated one (**TeSa2**). Also, in both cases, the *b*-forms with a O $\cdots$ H–Te or S $\cdots$ H–Te IHBs are close in energy to the aforementioned *a*-type structures. A quantitative analysis of the relative strengths of these intramolecular hydrogen bonds in terms of the isodesmic reactions 2 and 3 yields results systematically parallel to those discussed above for the corresponding selenium analogues (See Table 3). Indeed, our estimations show that the O–H $\cdots$ Te IHB is about 9 kcal mol<sup>-1</sup> stronger than the O $\cdots$ H–Te one (See Table 3), and again this difference is of the same order as the stability difference between *keto* and *enol* forms (See Table 2). Similarly, when oxygen is replaced by sulfur, both the S–H $\cdots$ Te and the S $\cdots$ H–Te IHBs become weaker and closer in stability, the energy gap between *thione* and *enethiol* forms being also rather small (3.5 kcal mol<sup>-1</sup>). Therefore, as far as the capacity of forming intramolecular hydrogen bonds with OH or SH groups, Se and Te behave quite similarly. Also in both the Se- and Te-series of compounds, the relative stability of *b*-type tautomers, stabilized by X $\cdots$ HTe IHBs, with respect to *a*-type ones, stabilized by XH $\cdots$ Te IHBs, is very similar. However, there is a dramatic difference as far as the chalcogen–chalcogen interactions are concerned. As mentioned above these interactions are weak in Se-containing compounds, but they are quite strong in Te-derivatives.

*Chalcogen–Chalcogen Interactions.* As pointed out in the paper of Minyaev and Minkin,<sup>30</sup> this interaction which received many different names, such as “premature hypervalent bond” or “fractional bond”, was traditionally associated with a n<sub>O</sub>– $\sigma^*_{\text{YH}}$  (or n<sub>S</sub>– $\sigma^*_{\text{YH}}$ ) dative bond involving the lone pairs of one of the chalcogen atoms (in our case oxygen or sulfur) and the  $\sigma^*_{\text{YH(Y=Se,Te)}}$  antibonding molecular orbital. As mentioned in the Introduction this picture seems to be consistent with the <sup>17</sup>O and <sup>77</sup>Se NMR spectroscopic characteristics of Se-containing compounds as shown recently by Komatsu et al.<sup>32</sup> Nevertheless, at least in the case of Te-derivatives, the electrostatic contributions cannot be neglected. To gain some insight into the physical origin of the aforementioned differences between Se- and Te-derivatives a more quantitative analysis of the weight of these two contributions is needed.

To estimate the weight of the electrostatic interaction we have evaluated the net atomic charges on both chalcogen groups by means of the NBO analysis.<sup>47</sup> With these values, and assuming a model of point charges located at the same relative position as the corresponding nuclei we have calculated the interaction energy between them. To estimate the weight of the n<sub>O</sub>– $\sigma^*_{\text{YH}}$  (or n<sub>S</sub>– $\sigma^*_{\text{YH}}$ ) dative bonding we have evaluated the corresponding orbital interaction by means of the second-order NBO analysis. Although the interaction energies so obtained (see Table 6) cannot be taken as an absolute measure of the electrostatic and covalent contributors, they allow us to estimate their relative importance in stabilizing the system. The first conspicuous fact of Table 6 is that both the electrostatic and the dative terms are much smaller in Se- than those in Te-derivatives. On the other hand, as expected from the high electronegativity of oxygen with respect to sulfur, the largest charge separation takes place in oxygen-containing compounds.

**TABLE 3: Energies of the Isodesmic Reactions 2 and 3 Evaluated at the G2(MP2) Level of Theory<sup>a</sup>**

Y = Se				Y = Te			
X = O		X = S		X = O		X = S	
reaction (2)	reaction (3)	reaction (2)	reaction (3)	reaction (2)	reaction (3)	reaction (2)	reaction (3)
12.2	2.9	6.1	4.5	10.3	1.0	5.8	3.0

<sup>a</sup> Values in kcal mol<sup>-1</sup>.**TABLE 4: Harmonic Vibrational Frequencies (cm<sup>-1</sup>) of Relevant Vibrational Modes of Vinylaldehydes (X = O, S, and Y = Se, Te)**

tautomer	X-H stretching	Y-H stretching	C-X stretching	C-Y stretching	X...Y stretching
<b>SeOa1</b>	2889		1375	718	213
<b>SeOa2</b>	3783		1349	896	
<b>SeOb3</b>		2326	1718	602	168
<b>SeOb2</b>		2370	1756	735	
<b>SeOb1</b>		2304	1721	640	134
<b>SeSa1</b>	1991		784	649	148
<b>SeSa2</b>	2672		776	892	
<b>SeSb3</b>		1909	1151	615	129
<b>SeSb2</b>		2372	1033	707	
<b>SeSb1</b>		2237	1137	614	131
<b>TeOa1</b>	3077		1401	585	180
<b>TeOa2</b>	3786		1324	748	
<b>TeOb3</b>		2105	1736	466	133
<b>TeOb2</b>		2049	1753	704	
<b>TeOb1</b>		1876	1630	588	171
<b>TeSa2</b>	2128		762	549	139
<b>TeSa1</b>	2675			694	
<b>TeSb3</b>		2084	1141	439	124
<b>TeSb2</b>		2050	1014	645	
<b>TeSb1</b>		1820	886	550	149

Also, reflecting the low electronegativity of Te, the electrostatic contribution is maximum when X = O and Y = Te. It is also worth noting that, although in Te-derivatives both electrostatic and dative interactions are large, our results indicate that in oxygen-containing systems the former clearly dominates, while the opposite is true in sulfur-containing species.

As it could be anticipated, the  $n_{\text{O}}-\sigma^*_{\text{YH}}$  (or  $n_{\text{S}}-\sigma^*_{\text{YH}}$ ) interaction results in a lengthening of the Y-H linkage due to the contribution of the  $\sigma^*_{\text{Y-H}}$  antibonding orbital. In line with our previous discussion this lengthening is greater in Te (0.033 Å for X = O and 0.051 for X = S) than that in Se-derivatives (0.010 Å for X = O and 0.020 for X = S), and it is also greater for sulfur than that for oxygen-containing compounds. Consistently the corresponding stretching frequencies appear red shifted as follows: (X = O, Y = Te) 173 cm<sup>-1</sup>; (X = S, Y = Te) 230 cm<sup>-1</sup>; (X = O, Y = Se) 66 cm<sup>-1</sup>; and (X = S, Y = Se) 135 cm<sup>-1</sup>. The charge donation from the lone pairs of the oxygen (or sulfur) atom also lengthens the C=O (or C=S) bond, because the oxygen (or the sulfur) recovers part of the charge transferred to the  $\sigma^*_{\text{YH}}$  orbital by depopulating the C=O (or C=S) bonding region. As a consequence, the charge density at the bond critical point decreases, the bond becomes longer (See Figure 1) and the stretching frequency appears red shifted (See Table 4).

It must be also emphasized that both effects are somehow interconnected, in the sense that the strong electrostatic attraction in Te-derivatives which results necessarily in short X-Te distances, strongly favors the donation from the lone pairs of X toward the Te-H  $\sigma^*$  antibonding orbital. This can be nicely visualized through the use of the contour maps of the energy density (See Figure 2). Indeed, in both selenium-derivatives the energy density curves associated with the valence regions of oxygen (or sulfur) and selenium do not overlap, while they

clearly do in the corresponding Te-derivatives, as a consequence of the short O-Te (and S-Te) distance. The main consequence is that in these two cases the energy density evaluated at the O...Te (or S...Te) bond critical points is negative, as in typical covalent linkages, reflecting a more efficient dative interaction. It is also important to note that these interactions are characterized by the existence of a bond critical point, whose charge density reflects the strength of the interaction (see Table 5), similarly to what was found for other weak bonds such as conventional hydrogen bonds.<sup>50-52</sup> Furthermore, the existence of a chalcogen-chalcogen bonding interaction implies that **SeOa1**, **SeSa1**, **TeOa1**, and **TeSa1** are formally cyclic structures, which is confirmed by the existence of a ring critical point (rcp) (see Table 5). It is worth noting that systematically the charge density at the rcp of the structures stabilized through a chalcogen-chalcogen interaction is higher than that of structures stabilized by IHBs, likely reflecting that in the former the ring is significantly more compact. It can be also observed that, within each subset, the higher the charge density at the rcp, the more stable is the isomer.

Finally, it is also worth mentioning that the chalcogen-chalcogen interaction in conformers, such as **SeOa3**, **SeSa3**, **TeOa3**, and **TeSa3**, are characterized by a repulsive electrostatic interaction, while in all cases the  $n_{\text{Y}}-\sigma^*_{\text{XH}}$  dative component does not take place. This means that when the chalcogen-chalcogen interaction involves C=Se (or C=Te) and OH (or SH) groups is not stabilizing.

Our efforts to have an unambiguous measure of the interaction energy and its components using the intermolecular case as a suitable reference failed. In principle, one may assume that the complexes between MeOH and TeCH<sub>2</sub> on one hand, and CH<sub>2</sub>O and CH<sub>3</sub>TeH on the other, would provide reasonable estimates of the strength of the O-H...Te IHB and the chalcogen-chalcogen O...TeH interaction, respectively. Furthermore, in the first case, depending on the relative orientation of the two moieties, with the H of the OH pointing toward or away from the Te atom, one may have a reasonable model to represent the kind of interactions present in **TeOa1** and **TeOa3** conformers. However, due to the fact that both interacting molecules are free to orient themselves in order to maximize the interaction energy, these two starting conformations collapsed to a unique structure (see Figure 3). This structure is stabilized through the formation of two hydrogen bonds. One of them involves the hydrogen atom of the OH group of methanol and the negatively charged carbon atom of TeCH<sub>2</sub>, and the other involves one of the positively charged hydrogen atoms of the TeCH<sub>2</sub> subunit and the oxygen of methanol. So while the rigidity of the corresponding  $\beta$ -chalcogenvinylaldehyde facilitates the O-H...Te interaction in the **TeOa1** compound, in the intermolecular case this interaction cannot compete with the stronger O-H...C and C-H...O hydrogen bonds.

In the case of interactions between CH<sub>2</sub>O and CH<sub>3</sub>TeH (See Figure 3) the corresponding complex is stabilized through a chalcogen-chalcogen interaction, but as it has been found before by Minyaev and Minkin<sup>30</sup>, there is also a contribution from a weak hydrogen bond between the Te-H group and the oxygen

**TABLE 5: Charge Densities ( $e\text{ au}^{-3}$ ) at Some Relevant Bond Critical Points (X = O, S, and Y = Se, Te) of the Different Chelated Conformers**

bond	SeOa1	SeOb3	SeOb1	SeSa1	SeSb3	SeSb1	TeOa1	TeOb3	TeOb1	TeSa2	TeSb3	TeSb1
C–X	0.320	0.390	0.392	0.213	0.223	0.226	0.285	0.363	0.339	0.206	0.223	0.219
C–Y	0.180	0.169	0.168	0.181	0.172	0.170	0.106	0.103	0.107	0.107	0.104	0.108
X–H	0.312			0.197			0.293			0.191		
Y–H		0.177	0.171		0.166	0.168		0.115	0.105		0.115	0.103
XH $\cdots$ Y	0.050			0.042			0.027			0.027		
X $\cdots$ HY		0.026			0.038			0.013			0.015	
X $\cdots$ Y			0.021			0.020			0.042			0.032
rcp <sup>a</sup>	0.014	0.011	0.015	0.011	0.010	0.013	0.012	0.009	0.022	0.009	0.007	0.016

<sup>a</sup> rcp = ring critical point.

**TABLE 6: Electrostatic and Covalent Contributions ( $\text{kcal mol}^{-1}$ ) to the Chalcogen–Chalcogen Interaction<sup>a</sup>**

SeOb1		SeSb1		TeOb1		TeSb1	
electro- static	dative	electro- static	dative	electro- static	dative	electro- static	dative
-2.01	-4.15	-0.10	-0.84	-15.18	-9.08	-1.30	-17.3

<sup>a</sup> These values should be taken in relative terms, not as a quantitative measure of the interaction in absolute terms (See text).

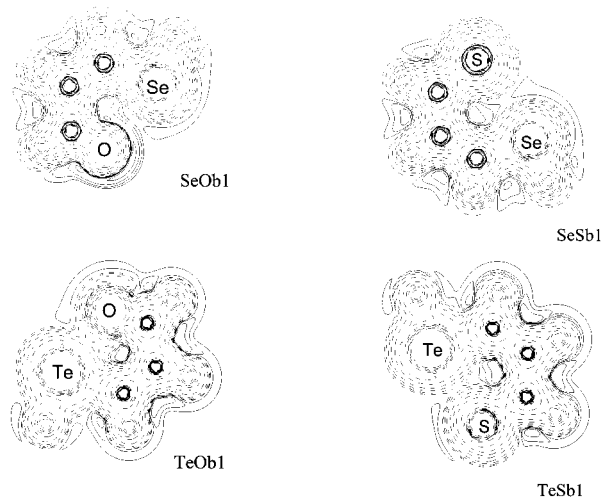


**Figure 2.** Contour maps of the energy density,  $H(r)$ , for **SeOb1**, **SeSb1**, **TeOb1**, and **TeSb1**. Dashed lines correspond to negative values and solid lines to positive values.

of formaldehyde, that prevents the separation of both components. Hence, a more quantitative analysis of the chalcogen–chalcogen interactions, as it is also the case for IHBs, is an open question which calls for additional studies.

**Proton-Transfer Barriers.** We have considered it of interest to investigate the proton-transfer mechanism that would connect in each case the two tautomers stabilized through an IHB because, as we have mentioned in the Introduction, these systems could be appropriate models to investigate ultrafast laser pulse isomerization-controlled mechanisms. According to our results we can distinguish two different situations: (a) systems which present a small energy barrier for the proton transfer, and as a consequence, either the ground vibrational state of the less stable isomer is above the energy barrier (as it is the case for **TeS-a2-b3** and **SeO-a1-b3**) or it is very close to it (as in **SeS-a1-b3**); (b) systems, such as **TeO-a1-b3**, which exhibit a reasonably high ( $>5\text{ kcal mol}^{-1}$ ) activation barrier. The formers are good examples, as some derivatives of TMA,<sup>18</sup> of low-barrier hydrogen bonds, which received a great deal of attention lately.<sup>53–55</sup> The latter is a good candidate to model proton-transfer isomerizations between the two isomers, **TeOa1** and **TeOb3** which are nearly degenerate.

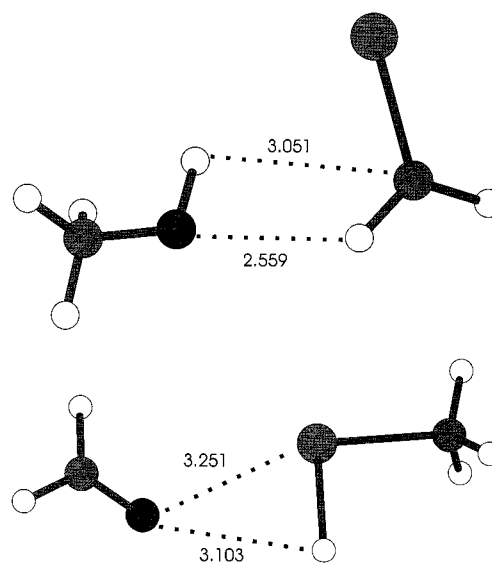


**Figure 3.** Equilibrium conformations of the complexes between  $\text{CH}_3\text{OH}$  and  $\text{CH}_2\text{Te}$  and between  $\text{CH}_2\text{O}$  and  $\text{CH}_3\text{TeH}$ , obtained at the B3LYP/6-31+G(d) level of theory.

## Conclusions

Our results indicate that in selenovinylaldehyde and selenothiovinylaldehyde the O–H $\cdots$ Se and the S–H $\cdots$ Se intramolecular hydrogen bonds compete in strength with the O $\cdots$ Se and the S $\cdots$ Se interactions, while the opposite is found for the corresponding tellurium-containing analogues. The different strength of O–H $\cdots$ Se and O $\cdots$ H–Se intramolecular hydrogen bonds explains why the chelated *enolic* and *keto* forms of selenovinylaldehyde are very close in energy, although *enol*-tautomers are estimated to be about  $10\text{ kcal mol}^{-1}$  more stable than *keto*-tautomers. The situation is qualitatively similar for selenothiovinylaldehyde, although the S–H $\cdots$ Se and S $\cdots$ H–Se intramolecular hydrogen bonds are weaker and much closer in strength, and the energy gap between *enethiol*- and *thione*-tautomers also smaller. Regarding the relative strengths of the X–H $\cdots$ Te and X $\cdots$ H–Te (X = O, S) IHBs, tellurium compounds behave very much as the corresponding selenium analogues. However, there are dramatic differences as far as the X $\cdots$ Y (X = O, S; Y = Se, Te) interactions are concerned, which for Se-derivatives they are rather small, while for Te-compounds they are very strong.

An analysis of these chalcogen–chalcogen interactions indicates that both the electrostatic and the dative contributions are smaller for Se– than for Te-derivatives. In the latter, the electrostatic component clearly dominates when X = O, while for sulfur-containing derivatives the donation from the lone pairs of sulfur to the Te–H  $\sigma^*$  antibonding orbital dominates. We have also shown that these two interactions are entangled in some manner, in the sense that strong electrostatic interactions

favor the  $n_{\text{O}}-\sigma^*_{\text{YH}}$  (or  $n_{\text{S}}-\sigma^*_{\text{YH}}$ ) dative interaction. The stabilizing chalcogen–chalcogen interactions can be characterized by the existence of a bond critical point, whose charge density reflects the strength of the interaction. Also the charge density at the ring critical point may provide information on the relative stability of the system.

**Acknowledgment.** This work has been partially supported by the D. G. I. Project No. BQU2000-0245. A generous allocation of computational time at the CCC of the Universidad Autónoma de Madrid is gratefully acknowledged.

## References and Notes

- (1) Jeffrey, G. A. *An Introduction to Hydrogen Bonding*; Oxford University Press: New York, 1997.
- (2) González, L.; Mó, O.; Yáñez, M. In *Recent Theoretical and Experimental Advances in Hydrogen Bonded Clusters*; Xantheas, S. S., Ed.; Kluwer Academic Publishers: Dordrecht, 2000.
- (3) Emsley, J. *Structure and Bonding*; Springer-Verlag: Berlin, 1984.
- (4) Frisch, M. J.; Scheiner, A. C.; Schaefer, H. F., III; Binkley, J. S. *J. Chem. Phys.* **1985**, *82*, 4194.
- (5) Sim, F.; St-Amant, A.; Papai, I.; Salahub, D. R. *J. Am. Chem. Soc.* **1992**, *114*, 4391.
- (6) Latajka, Z.; Scheiner, S. *J. Phys. Chem.* **1992**, *96*, 9764.
- (7) Mulhearn, D. C.; Bachrach, S. *J. Org. Chem.* **1995**, *60*, 7110.
- (8) Barone, V.; Adamo, C. *J. Chem. Phys.* **1996**, *105*, 11007.
- (9) Mó, O.; Yáñez, M.; Esseffar, M.; Herreros, M.; Notario, R.; Abboud, J. L. M. *J. Org. Chem.* **1997**, *62*, 3200.
- (10) Bouchoux, G.; Defaye, D.; McMahon, T.; Mó, O.; Yáñez, M. *Chemistry Eur. J.* In press.
- (11) Bouchoux, G.; Gal, J. F.; Maria, P. C.; Szulejko, J. E.; McMahon, T. B.; Tortajada, J.; Luna, A.; Yáñez, M.; Mó, O. *J. Phys. Chem. A* **1998**, *102*, 9183.
- (12) Jackman, L. M.; Trewella, T. E.; Haddon, R. C. *J. Am. Chem. Soc.* **1980**, *102*, 2519.
- (13) Redington, R. L.; E., R. T.; Hunter, M. A.; Field, R. W. *J. Chem. Phys.* **1990**, *92*, 6456.
- (14) Ríos, M. A.; Rodríguez, J. *Can. J. Chem.* **1991**, *69*, 201.
- (15) Tsuji, T.; Sekiya, H.; Nishimura, Y.; Mori, R.; Mori, A.; Takeshita, H. *Chem. Phys.* **1992**, *97*, 6032.
- (16) Frost, R. K.; Hagemester, F. C.; Arrington, C. A.; Zwier, T. S.; Jordan, K. D. *J. Chem. Phys.* **1996**, *105*, 2595.
- (17) González, L.; Mó, O.; Yáñez, M. *J. Phys. Chem. A* **1997**, *101*, 9710.
- (18) González, L.; Mó, O.; Yáñez, M. *J. Org. Chem.* **1999**, *64*, 2314.
- (19) Duus, F. *J. Org. Chem.* **1977**, *42*, 3123.
- (20) Jorgensen, F. S.; Carlsen, L.; Duus, F. *J. Am. Chem. Soc.* **1981**, *103*, 1350.
- (21) Berg, U.; Sandström, J.; Carlsen, L.; Duus, F. *J. Chem. Soc., Perkin Trans. 2* **1983**, 1321.
- (22) Duus, F. *J. Am. Chem. Soc.* **1986**, *108*, 630.
- (23) Doslic, N.; Sundermann, K.; González, L.; Mó, O.; Giraud-Girard, J.; Kühn, O. *Phys. Chem. Chem. Phys.* **1999**, *1*, 1249.
- (24) Doslic, N.; Kühn, O.; Manz, J.; Sundermann, K. *J. Phys. Chem.* **1998**, *102*, 9645.
- (25) Doslic, N.; Kühn, O.; Manz, J. *Ber. Bunsen-Ges. Phys. Chem.* **1998**, *102*, 1.
- (26) Ammal, S. S. C.; Venuvanalingam, P. *J. Phys. Chem. A* **2001**, *104*, 10859.
- (27) Adcock, N. M. *Adv. Inorg. Chem. Radiochem.* **1972**, *15*, 1.
- (28) Angyan, G.; Poirier, R. A.; Kucsman, A.; Csizmadia, I. G. *J. Am. Chem. Soc.* **1987**, *109*, 2237.
- (29) Burgi, H.-B.; Dunitz, J. *J. Am. Chem. Soc.* **1987**, *109*, 2924.
- (30) Minyaev, R. M.; Minkin, V. I. *Can. J. Chem.* **1998**, *76*, 776.
- (31) Minkin, V. I.; Minyaev, R. M. *Chem. Rev.* **2001**, *101*, 1247.
- (32) Komatsu, H.; Iwaoka, M.; Tomoda, S. *Chem. Commun.* **1999**, 205.
- (33) Takaguchi, Y.; Hosokawa, A.; Yamada, S.; Motoyoshiya, J.; Aoyama, H. *J. Chem. Soc., Perkin Trans. 1* **1998**, 3147.
- (34) Curtiss, L. A.; Raghavachari, K.; Pople, J. A. *J. Chem. Phys.* **1993**, *98*, 1293.
- (35) Curtiss, L. A.; McGrath, M. P.; Blaudeau, J.-P.; Davis, N. E.; Binning, R. C., Jr.; Radom, L. *J. Chem. Phys.* **1995**, *103*, 6104.
- (36) Glukhovtsev, M. N.; Pross, A.; McGrath, M. P.; Radom, L. *J. Chem. Phys.* **1995**, *103*, 1878.
- (37) González, A. I.; Mó, O.; Yáñez, M. *J. Chem. Phys.* **2000**, *112*, 2258.
- (38) Gal, J.-F.; Decouzon, M.; Maria, P.-C.; González, A. I.; Mó, O.; Yáñez, M.; El Chaouch, S.; Guillemin, J.-C. *J. Am. Chem. Soc.* **2001**, *123*, 6353.
- (39) Stevens, W. J.; Krauss, M.; Basch, H.; Jasien, P. G. *Can. J. Chem.* **1992**, *70*, 612.
- (40) Curtiss, L. A.; Raghavachari, K.; Trucks, G. W.; Pople, J. A. *J. Chem. Phys.* **1991**, *94*, 7221.
- (41) Flaud, J. M.; Arcas, P.; Burger, H.; Polanz, O.; Halonen, L. *J. Mol. Spectrosc.* **1997**, *183*, 310.
- (42) Becke, A. D. *J. Chem. Phys.* **1988**, *88*, 1053.
- (43) Becke, A. D. *J. Chem. Phys.* **1993**, *98*, 5648.
- (44) Becke, A. D. *J. Chem. Phys.* **1993**, *98*, 1372.
- (45) Lee, C.; Yang, W.; Parr, R. G. *Phys. Rev. B: Condens. Matter* **1988**, *37*, 785.
- (46) Bader, R. F. W. *Atoms in Molecules. A Quantum Theory*; Clarendon Press: Oxford, 1990.
- (47) Reed, A. E.; Curtiss, L. A.; Weinhold, F. *Chem. Rev.* **1988**, *88*, 899.
- (48) Cremer, D.; Kraka, E. *Angew. Chem.* **1984**, *96*, 612.
- (49) González, A. I.; Mó, O.; Yáñez, M. *J. Phys. Chem. A* **1999**, *103*, 1662.
- (50) Mó, O.; Yáñez, M.; Elguero, J. *J. Chem. Phys.* **1992**, *97*, 6628.
- (51) Alkorta, I.; Rozas, I.; Elguero, J. *Struct. Chem.* **1998**, *9*, 243.
- (52) Alkorta, I.; Elguero, J. *J. Phys. Chem. A* **1999**, *103*, 272.
- (53) García-Viloca, M.; Gelabert, R.; González-Lafont, A.; Moreno, M.; Lluch, J. M. *J. Am. Chem. Soc.* **1998**, *120*, 10203.
- (54) Cleland, W. W.; Kreevoy, M. M. *Science* **1995**, *269*, 104.
- (55) Cassidy, C. S.; Lin, J.; Frey, P. A. *Biochem.* **1997**, *36*, 4576.